Journal of Southeast University (English Edition) Vol. 25, No. 4, pp. 506 – 512 Dec. 2009 ISSN 1003—7985

# Seismic strengthening of reinforced concrete columns damaged by rebar corrosion using combined CFRP and steel jacket

Li Jinbo Gong Jinxin

(State Key Laboratory of Coastal and Offshore Engineering, Dalian University of Technology, Dalian 116024, China)

**Abstract:** In order to study the effectiveness of combined carbon fiber-reinforced polymer (CFRP) sheets and steel jacket in strengthening the seismic performance of corrosion-damaged reinforced concrete (RC) columns, twelve reinforced concrete columns are tested under combined lateral cyclic displacement excursions and constant axial load. The variables studied in this program include effects of corrosion degree of the rebars, level of axial load, the amount of CFRP sheets and steel jacket. The results indicate that the combined CFRP and steel jacket retrofitting technique is effective in improving load-carrying, ductility and energy absorption capacity of the columns. Compared with the corrosion-damaged RC column, the lateral load and the ductility factor of many strengthened columns increase more than 90% and 100%, respectively. The formulae for the calculation of the yielding load, the maximum lateral load and the displacement ductility factor of the strengthened columns under combined constant axial load and cyclically increasing lateral loading are developed. The test results are also compared with the results obtained from the proposed formulae. A good agreement between calculated values and experimental results is observed.

**Key words:** reinforced concrete column; seismic performance; corrosion; retrofitting; steel jacket; fiber-reinforced polymer (FRP); ductility

Many existing reinforced concrete (RC) structures damaged by corrosion may have inadequate seismic resistance due to the loss of the reinforcing steel cross-sectional area as well as the loss of bond along the steel-concrete interface. As a result, many of these structures suffer extensive structural damage and even collapse when subjected to a strong ground motion[1-4]. Therefore, it is necessary to clarify the influence of rebar corrosion and strengthen the damaged column in order to upgrade the seismic performance of damaged structures.

There are considerable research efforts being directed at developing and applying retrofit strategies to upgrade the seismic performance of deficient structures. Externally bonded fiber-reinforced polymers (FRP), as a promising rehabilitation system to upgrade damaged RC columns, have been examined in much of the literature[4-5]. The researches have proved the ability of the FRP system to improve the ductility and energy absorption capacity of corroded RC columns, but the FRP system cannot significantly improve the strength of the corroded RC column. Steel jacketing, as a conventional strengthening technique, can improve the bending strength, the shear capacity, the stiffness, the ductility and the axial load carrying capacity of strengthened elements[6-7], but the strengthening technique is not suitable for strengthening the corroded RC column because the steel jacket may be damaged by marine environments and deicing salts.

Although a variety of strengthening methods are used to strengthen the damaged column, currently no attempts have been made to strengthen the corroded RC column with combined CFRP sheets and steel jacketing. Thus, a study is made in this program in order to make full use of the advantages of the two kinds of materials in improving the seismic performance of the RC column.

## 1 Experimental Program

### 1.1 Specimen details

Twelve RC columns are constructed and tested under combined axial load and reversed cyclic lateral displacement excursions. As shown in Fig. 1, the original columns have a clear height of 1 500 mm with a cross section of 200 mm × 200 mm. Four 14-mm diameter bars are used as longitudinal reinforcement, stirrups of 8-mm diameter bars are spaced at every 100 mm and have 135° hooks at the ends. Three 150 mm × 150 mm × 150 mm cubes are cast along with the specimens, and the 28-day mean cube compressive strength is 44.8 MPa. The other details of the specimens are shown in Fig. 1. The black region in which the length is 500 mm in Fig. 1(c) is the region wrapped with CFRP sheets. The repair procedure of the specimens in Fig. 1(c) consists of bonding steel jacketing first and then wrapping CFRP sheets.

### 1.2 Accelerated steel corrosion test

The external current method is used to induce corrosion in the columns after a 28 d curing[8], as shown in Fig. 2. The specimens are placed in a water tank containing 3.5% salt solution. A reinforcement cage of each specimen is used as the anode and corrosion resistant plates immersed in the bank are used as the cathode. The current and the voltage in each column are measured periodically. To achieve the same level of corrosion in all columns, the current in each column is tuned so that areas under the current-time plots for specimens are similar. Tab. 1 gives the weight loss of the rebars corresponding to different corrosion degrees. The appearances of the columns at the end of the accelerated corrosion process are given in Fig. 3.

At the termination of the corrosion process, longitudinal splitting cracks are running parallel to the steel reinforcing bars for all corroded specimens. In addition to the cracks, many red-black corrosion products, which are concentrated on or close to the corrosion cracks, are observed leaching out of the cracks. This phenomenon implies that rendering

**Received** 2009-01-06.

**Biographies:** Li Jinbo (1981—), male, doctor; Gong Jinxin (corresponding author), male, doctor, professor, gong_jx.vip@eyou.com.

**Foundation item:** The Program for Changjiang Scholars and Innovative Research Team in University of Ministry of Education of China (No. IRT0518).

**Citation:** Li Jinbo, Gong Jinxin. Seismic strengthening of reinforced concrete columns damaged by rebar corrosion using combined CFRP and steel jacket[J]. Journal of Southeast University (English Edition), 2009, 25 (4): 506 – 512.

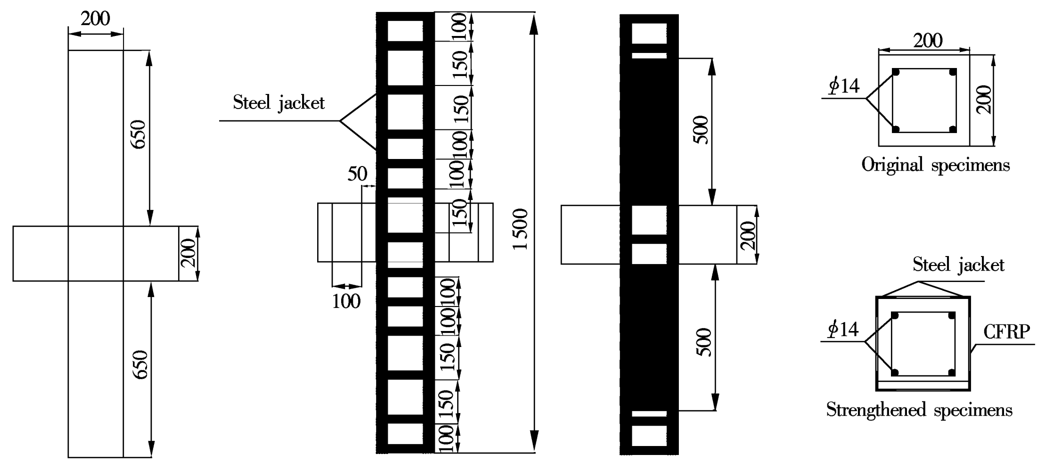


**Fig. 1** Geometrical size of the strengthened column( unit: mm)

the structural behaviors of the RC column have been damaged due to serious rust stains and concrete deterioration.

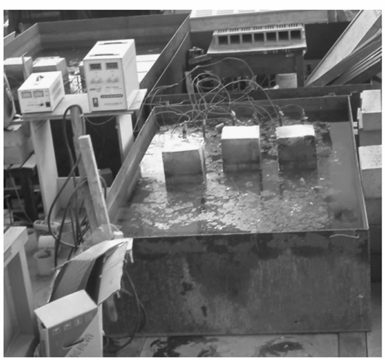

**Fig. 2** Experimental device of the accelerated corrosion of rebars by the electrochemical method

**Fig. 3** Columns after rebar corrosion

**Tab. 1** Configuration of specimens

| Specimens | Corrosion loss ratio/% | Axial load/kN | Strengthening methods |
|---|---|---|---|
| RA0 | 0 | 420 | Sound specimen |
| RBJ121 | 19. 56 | 180 | Steel jacket + 1 layer of CFRP sheet |
| RB2 | 19. 17 | 300 | Unstrengthened |
| RBJ22 | 16. 50 | 300 | Steel jacket |
| RBJ221 | 18. 80 | 300 | Steel jacket + 1 layer of CFRP sheet |
| RBJ222 | 17. 20 | 300 | Steel jacket + 2 layers of CFRP sheets |
| RBJ223 | 16. 89 | 300 | Steel jacket + 1 layer of CFRP sheet |
| RB3 | 16. 80 | 420 | Unstrengthened |
| RBJ321 | 16. 70 | 420 | Steel jacket + 1 layer of CFRP sheet |
| RC2 | 11. 49 | 300 | Unstrengthened |
| RCJ22 | 9. 90 | 300 | Steel jacket |
| RCJ221 | 9. 30 | 300 | Steel jacket + 1 layer of CFRP sheet |

## 1. 3 Strengthening process

Eight of the corroded specimens described above are strengthened when the specimens reach the destined corrosion ratio. The repair process consists of removing deteriorated concrete, cleaning the corroded reinforcing steel, casting repair material, and strengthening the columns with different retrofitting methods. The repair material is a normal strength concrete with a 28-day compressive strength of 32. 7 MPa. Two strengthening techniques are used and Tab. 1 gives the details. It is noticed that, for the specimens strengthened with combined CFRP sheets and steel jacket, the steel jacket is bonded with epoxy resin first and then epoxy based mortar is applied as screed-coat before wrapping the CFRP sheets.

The steel jacket, which is used for strengthening the corroded specimens, consists of four steel angles. The cross-section of steel angle in specimen RBJ223 is 30 mm × 30 mm × 3 mm, but that in other specimens is 40 mm × 40 mm × 4 mm. Four steel angles are welded by batten plates with a cross-section of 30 mm × 3 mm and by a space of 150 mm. The mechanical characteristics of the steel rebars, steel angle and batten plates are given in Tabs. 2 and 3.

**Tab. 2** Mechanical properties of steel rebars

| Element | Bar diameter/mm | Yield stress/MPa | Ultimate stress/MPa |
|---|---|---|---|
| Longitudinal reinforcement | 14 | 384. 77 | 604. 87 |
| Stirrups | 8 | 326. 95 | 510. 70 |

**Tab. 3** Mechanical properties of steel angle

| Element | Cross-section | Yield stress/MPa | Ultimate stress/MPa |
|---|---|---|---|
| Steel jacket 1 | 40 mm × 40 mm × 4 mm | 350 | 458. 3 |
| Steel jacket 2 | 30 mm × 30 mm × 3 mm | 338. 5 | 461. 5 |
| Batten plate | 30 mm × 3 mm | 533. 3 | 666. 7 |

For the specimens strengthened with combined CFRP sheets and steel jacket, the corners of each column are rounded to a radius of 20 mm and CFRP sheets are wrapped around the whole test region in a peripheral direction with a 200 mm overlap. It is noticed that, except for the specimen

RBJ222 wrapped with two layers of CFRP sheets, all the other specimens have only one layer of CFRP sheet. Tab. 4 gives the material properties of the CFRP sheet.

**Tab. 4** Material properties of CFRP

| Sheet thickness/mm | Tensile strength/GPa | Tensile modulus/GPa | Tensile elongation/% |
|---|---|---|---|
| 0. 111 | 3. 646 | 215. 6 | 1. 9 |

### 1. 4 Test setup

Fig. 4 shows the loading frame and part of the instrumentation used for the lateral load tests. The top and bottom of each column are fixed by the test frame using the bolts and a ball socket bearing is placed under the bottom of the column. Axial load, given in Tab. 1, is first applied using hydraulic loading equipment and remains constant during the testing process to simulate the dead load on the column. The reversed cyclic lateral load is then applied through two one-way hydraulic jacks and measured by two load cells attached to the hydraulic jacks. The displacement control mode is used to apply the predetermined displacement history, which means that the specimen is subjected to a displacement of $\Delta_1 = 1$ mm for the first cycle followed by three cycles, each of $2\Delta_1$, $4\Delta_1$, $6\Delta_1$, ..., until the column fails, as shown in Fig. 5.

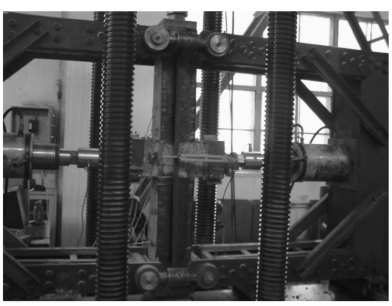

**Fig. 4** Test setup for column testing

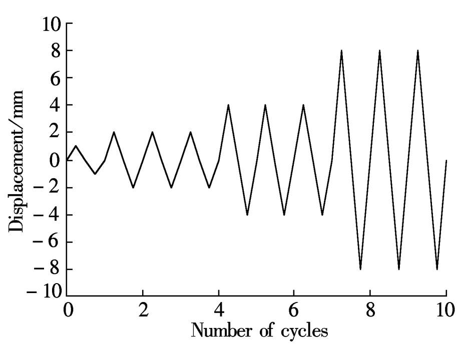


**Fig. 5** Lateral displacement history

## 2 Test Results

Three control specimens (RB2, RB3 and RC2), which have different corrosion levels, are tested to failure without any strengthening to establish the behavior against which the performance of the strengthened specimens can be evaluated. Since they have similar failure mechanisms, specimen RB3 is selected as a representative sample. Specimen RB3 has four longitudinal corrosion cracks due to rebar corrosion before loading and the longitudinal cracks continue to develop as the lateral load increases. This is followed by the appearance of flexural cracks at the interval within 300 mm from the stub interface, during the second cycle ($\delta_{max} = 2\Delta_1$). From the third cycle($\delta_{max} = 4\Delta_1$) onward, all the cracks continue to grow and lead to initiation of spalling of the concrete near the column-stub interface. During the last cycles, the concrete cover falls off completely. From this observation on the specimen after failure, it is concluded that the falling off of the concrete cover is caused by the corrosion of the rebar, which reduces the bond between the concrete cover and the core.

Specimens RBJ22 and RCJ22 are strengthened with steel jacketing only, so specimen RBJ22 is selected as a representative sample. The behavior of specimen RBJ22 is characterized by stable hysteretic hoops in both directions of loading due to confinement of the steel jacket. The maximum load is 265. 79 kN and the corresponding displacement is 8 mm. From the ninth cycle ($\delta_{max} = 16\Delta_1$) onward, the connection between steel angle and batten plate near the column-stub interface is ruptured and results in considerable degradation of flexural strength of the column.

Other specimens except RA0, strengthened with combined CFRP sheets and steel jacket show similar behavior. Hence specimen RBJ321 is chosen as a representative sample. The specimen RBJ321 exhibits more stable behavior than the columns strengthened only with steel jacketing due to the confinement of combined CFRP sheets and the steel jacket. There is a distinct yield plateau followed by a gradual hardening up to a maximum load, followed by gradual softening after the maximum load. During the 11th cycle ($\delta_{max} = 20\Delta_1$), the rupture of the steel angle near the location of the column-stub interface occurs and results in rapid degradation of the flexural strength of the column, and the test is terminated.

Fig. 6 gives the views of failure of some specimens and Fig. 7 gives the lateral load against displacement curves for some specimens. Tab. 5 summarizes the results of the cyclic tests. $P_y$ and $\Delta_y$ are the yield load and corresponding displacement, respectively. $P_{max}$ is the maximum applied lateral load and $\Delta_{max}$ is the corresponding displacement. $P_u$ is the failure load, which is defined as 85% of the maximum lateral load $P_{max}$, and $\Delta_u$ is the corresponding failure displacement. $\mu_\Delta$ is the displacement ductility factor, calculated by $\Delta_u/\Delta_y$, $E_{end}$ is the total cumulative dissipated energy.

(a) (b)

**Fig. 6** Views of failure of the specimens. (a) RBJ22; (b) RBJ321

**Tab. 5** List of the test results

| Specimen | $P_y$/kN | $\Delta_y$/mm | $P_{max}$/kN | $\Delta_{max}$/mm | $P_u$/kN | $\Delta_u$/mm | $\mu_\Delta$ | $E_{end}$/(kN · m) |
|---|---|---|---|---|---|---|---|---|
| RA0 | 160.66 | 2.10 | 190.87 | 6.10 | 162.24 | 7.50 | 3.60 | 5.23 |
| RBJ121 | 223.71 | 2.45 | 253.60 | 8.60 | 215.56 | 18.40 | 7.51 | 79.70 |
| RB2 | 153.10 | 1.90 | 164.91 | 6.30 | 140.17 | 6.80 | 3.58 | 4.44 |
| RBJ22 | 220.21 | 2.75 | 265.79 | 8.17 | 225.92 | 18.02 | 6.55 | 78.70 |
| RBJ221 | 265.68 | 2.73 | 316.45 | 9.95 | 268.98 | 19.90 | 7.29 | 116.98 |
| RBJ222 | 253.14 | 2.45 | 291.17 | 14.45 | 247.49 | 26.50 | 10.80 | 221.24 |
| RBJ223 | 172.43 | 2.05 | 234.31 | 4.25 | 199.16 | 22.71 | 11.08 | 78.89 |
| RB3 | 135.20 | 1.60 | 173.20 | 3.10 | 147.22 | 4.74 | 2.96 | 3.73 |
| RBJ321 | 262.57 | 3.00 | 334.68 | 12.64 | 284.47 | 19.76 | 6.58 | 81.92 |
| RC2 | 135.42 | 2.60 | 167.80 | 8.10 | 142.63 | 12.23 | 4.70 | 8.59 |
| RCJ22 | 230.58 | 3.60 | 279.62 | 10.33 | 237.68 | 22.90 | 6.36 | 104.87 |
| RCJ221 | 272.14 | 3.00 | 320.64 | 12.28 | 272.54 | 19.49 | 6.47 | 117.00 |

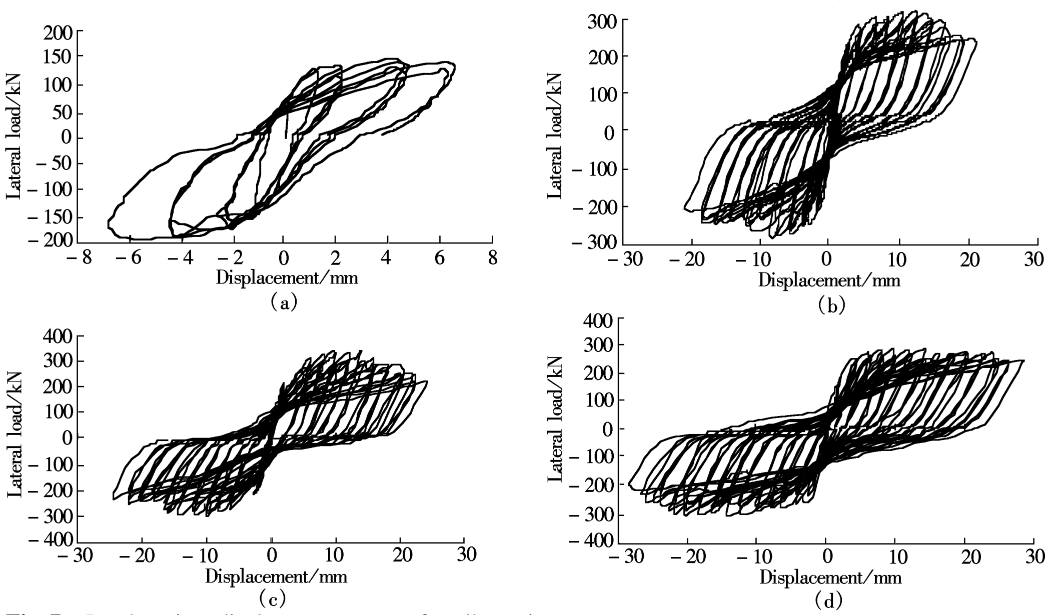


**Fig. 7** Load against displacement curves for all specimens. (a) RB2; (b) RBJ22; (c) RBJ221; (d) RBJ222

## 3 Discussion

### 3.1 Lateral load-displacement response

Ductility factors and lateral loads are two of the most common parameters used for the seismic evaluation of structural components. In Fig. 8, the envelopes of the lateral load-displacement response of all test specimens are compared with rebar corrosion, CFRP layers, axial load level and steel jackets on the ductility factors and lateral loads of the specimens.

It can be seen from Fig. 8 that, the enhancement in displacement ductility factors is found to be larger for specimens RBJ22 and RBJ221, which are tested with larger corrosion degrees, than the corresponding enhancements for specimens RCJ22 and RCJ221, which are tested with lower corrosion degrees. The reason for this behavior is that, although the steel jacket or combined CFRP and steel jacket reduces the bond degradation of the corroded rebars, but the specimen RB2 exhibits poorer displacement ductility than specimen RC2 due to the greater degree of corrosion.

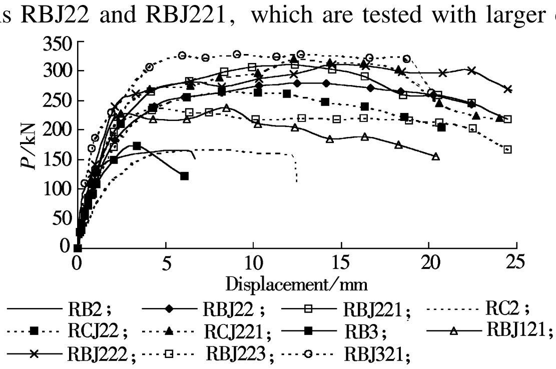


**Fig. 8** Lateral force-displacement response envelopes

The effect of axial load on the cyclic behavior of the strengthened columns with combined CFRP sheet and steel jacketing can also be evaluated in Fig. 8. The enhancements in the maximum lateral load and the ductility factor are higher for specimen RBJ321, which is tested under a high axial load, with the maximum lateral load value and the ductility factor value increasing 93.2% and 122.3%, respectively, than those with corresponding values of control specimen RB3. Corresponding enhancements in the maximum lateral load value and the ductility factor value for specimen RBJ221 are 91.9% and 103.6%, respectively, than for those of specimen RB2. This is because under low axial load, both the strengthened and control specimens are able to sustain a large number of cyclic excursions; the strengthened columns do so with gradual degradation of strength while the strength degradation in control columns is more severe, but for the specimens tested under high axial load, the control specimen undergoes rapid degradation of strength and fails much earlier than the strengthened specimen.

Fig. 8 also shows the effect of CFRP sheets on the ductility and lateral load of specimens. By comparing the results of the specimens, it is evident that, strengthening of the columns with combined CFRP and steel jacketing or steel jacketing results in more stable responses with larger strength and ductility. The improvements are found to be much greater in the specimens strengthened with combined CFRP and steel jacketing than in the specimens strengthened only with steel jacketing due to CFRP wraps. It is due to the confinement of concrete in the plastic hinge regions. Confining the strengthened column using steel jacketing with one or two layers of FRP helped to delay the formation of internal splitting cracks between the corroded columns and the steel jacket, thus improving the seismic behavior of the strengthened columns.

### 3. 2 Energy absorption capacities

Fig. 9 shows the total cumulative dissipated energies for the specimens. The total cumulative dissipated energy is calculated from the sum of the energy absorbed in all cycles before the specimens failed.

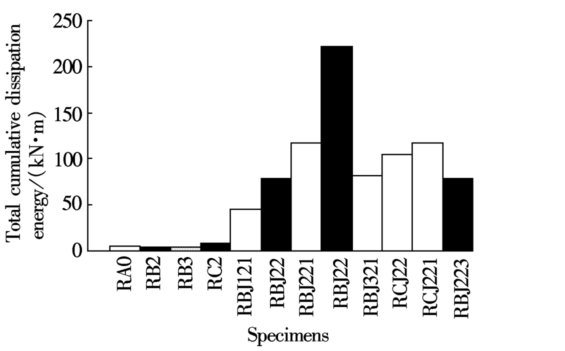


**Fig. 9** Total cumulative energy absorption for all specimens

It can be seen from Fig. 9 that, integration of the total hysteretic energy absorbed by the columns indicates that the retrofitted columns are capable of absorbing more energy than that of the corroded columns before the columns fail. It can also be seen that the CFRP confinement substantially improves the energy absorption and dissipation capacities of the specimens strengthened with steel jacketing. Increasing the area of CFRP from zero to two layers results in a sizable increase in the energy absorption capacity.

## 4 Analytical Studies

### 4. 1 Yield force and the maximum lateral load calculations of the strengthened specimens

According to the test results, the strengthened specimens fail in the flexural mode. Thus, the yield force and the maximum lateral load are obtained from the flexural strength of the bottom section of the column. The tension reinforcement in the original column is considered by multiplying the reduced factor of 0. 8. This is because the bond force between the reinforcement and concrete is reduced due to the back-filled concrete cover.

The yield moment and yield load of the strengthened columns are calculated by

$$M_y = 0.8 f_y A_s (1 - p)(h_0 - a_0) + 0.5 N h (1 - n_0) + k A_a f_{ay} h \tag{1}$$

$$P_y = \frac{M_y}{H} \tag{2}$$

where $M_y$ is the yield moment of the strengthened columns; $P_y$ is the yield load of the strengthened columns; $f_y$ is the yield strength of the longitudinal bars; $A_s$ is the area of the longitudinal bars; $h_0$ is the effective depth of the column; $a_0$ is the depth of concrete cover; $p$ is the corrosion ratio of the longitudinal bars; $N$ is the axial load; $n_0$ is the axial load ratio; $n_0 = N/(f_c bh)$; $k$ is the effectiveness factor of the steel jacket. For the column strengthened only with steel jacketing, $k = 0.7$, for the column strengthened both with CFRP and steel jacket, $k = 0.8$; $A_a$ is the area of tensile steel angle; $f_{ay}$ is the yield strength of the tensile steel angle, and $H$ is the shear span of the column.

According to Ref. [9], the maximum lateral loads $P_{max}$ of the columns are calculated by

$$P_{max} = (1.24 - 0.15\rho - 0.5 n_0) P_y \tag{3}$$

where $\rho$ is the tension steel ratio, $\rho = \rho_1 + \rho_2$, $\rho_1$ is the tension longitudinal steel ratio and $\rho_2$ is the tension steel angle ratio.

The comparison between test values with calculated values of the yield loads and the maximum lateral loads of the strengthened columns are shown in Tab. 6. In Tab. 6, $P_{yt}$ and $P_{maxt}$ are the test values of the yield loads and the maximum lateral loads of the column, respectively; $P_{yc}$ and $P_{maxc}$ are the calculated values of the yield loads and the maximum lateral loads of the column, respectively. Comparing the test values with the calculated values of the yield loads and the maximum lateral loads, it can be seen that the test results of the yield loads and the maximum lateral loads of the strengthened columns agree well with the corresponding calculated values.

**Tab. 6** Comparison of yield load and maximum lateral load

| Specimen | $P_{yt}$/kN | $P_{yc}$/kN | $P_{yc}/P_{yt}$ | $P_{maxt}$/kN | $P_{maxc}$/kN | $P_{maxc}/P_{maxt}$ |
|---|---|---|---|---|---|---|
| RBJ121 | 223. 71 | 229. 60 | 1. 03 | 253. 60 | 268. 75 | 1. 06 |
| RBJ22 | 220. 21 | 232. 66 | 1. 06 | 265. 79 | 266. 08 | 1. 00 |
| RBJ221 | 265. 68 | 258. 25 | 0. 97 | 316. 45 | 290. 90 | 0. 92 |
| RBJ222 | 253. 14 | 259. 07 | 1. 02 | 291. 17 | 291. 82 | 1. 00 |
| RBJ223 | 172. 43 | 199. 10 | 1. 15 | 234. 31 | 224. 46 | 0. 96 |
| RBJ321 | 262. 57 | 279. 90 | 1. 07 | 334. 68 | 302. 95 | 0. 91 |
| RCJ22 | 230. 58 | 239. 60 | 1. 04 | 279. 62 | 269. 89 | 0. 97 |
| RCJ221 | 272. 14 | 263. 12 | 0. 97 | 320. 64 | 296. 39 | 0. 92 |

### 4.2 Ductility factor calculations of the strengthened specimens

Ductility factor is one of the most common parameters used for the seismic evaluation of structural components. In order to evaluate the performance of the columns under the current research, the displacement ductility factors $\mu_\Delta$ of the strengthened columns are used. Based on the test results, the displacement ductility factors $\mu_\Delta$ of the strengthened columns are calculated by

$$\mu_\Delta = \frac{\sqrt{1 + 20\alpha_w \lambda_w}}{0.045 + 1.1 n_0} \tag{4}$$

where $\alpha_w$ is a factor representing the type of hoops, $\alpha_w = 1.0$ for square hoops; $\lambda_w$ is the equivalent transverse reinforcement index for the confinement from steel hoops, wrapped CFRP and steel jacketing, and it can be expressed as $\lambda_w = \rho_{w1}\alpha_{f1} + \nu_2\rho_{w2}\alpha_{f2} + \nu_3\rho_{w3}\alpha_{f3}$. Here $\rho_{w1}$, $\rho_{w2}$ and $\rho_{w3}$ are the volume ratios of stirrups, CFRP and batten plate to the confined concrete, respectively; $\alpha_{f1}$, $\alpha_{f2}$ and $\alpha_{f3}$ are the ratios of the yield strength of stirrups, the tensile strength of CFRP and the yield strength of batten plate to the equivalent compressive strength of concrete $f_c$, respectively. $\nu_2$ and $\nu_3$ are the effective confinement factors of CFRP and batten plate, respectively. $\nu_2 = \varepsilon_{cf}/\varepsilon_{cu}$, $\varepsilon_{cf}$ is the average CFRP strain in the plastic hinge zone of the column at the ultimate lateral displacement $\Delta_u$, and $\varepsilon_{cu}$ is the rupture strain of CFRP. $\nu_3 = \varepsilon_{af}/\varepsilon_{au}$, $\varepsilon_{af}$ is the average strain of batten plate in the plastic hinge zone of the column at the ultimate lateral displacement $\Delta_u$ and $\varepsilon_{au}$ is the strain of batten plate corresponding to the yield strength of batten plate. Based on the test results, $\nu_2 = 0.45$, $\nu_3 = 0.35$.

Tab. 7 shows the comparison between the test values with the calculated values of the displacement ductility factors of the strengthened columns. In Tab. 7, $\mu_{\Delta t}$ and $\mu_{\Delta c}$ are the test displacement ductility factors and calculated displacement ductility factors of the strengthened columns, respectively.

Compared the calculated values with the test values of the displacement ductility factors in Tab. 7, it can be seen that, except for the specimens RBJ121 and RBJ221, all the other calculated results are within a 17% error band. This error band scope is allowable for calculating the displacement ductility factor of strengthened columns. Thus, the calculated results confirm the ability of the proposed calculation method to predict the displacement ductility factor of strengthened columns.

**Tab. 7** Comparison of displacement ductility factor

| Specimen | $\mu_{\Delta t}$ | $\mu_{\Delta c}$ | $\left\lvert \frac{\mu_{\Delta c} - \mu_{\Delta t}}{\mu_{\Delta t}} \right\rvert$/% |
|---|---|---|---|
| RBJ121 | 7.51 | 11.06 | 47 |
| RBJ22 | 6.55 | 5.99 | 9 |
| RBJ221 | 7.29 | 7.65 | 5 |
| RBJ222 | 10.80 | 9.00 | 17 |
| RBJ223 | 11.08 | 7.91 | 29 |
| RBJ321 | 6.58 | 5.69 | 14 |
| RCJ22 | 6.36 | 5.91 | 7 |
| RBJ221 | 6.47 | 7.57 | 17 |

## 5 Conclusions

The effectiveness of strengthening damaged RC columns using combined CFRP sheets and steel jacketing to improve the seismic performance of RC columns has been examined in this paper. Based on the research results, the following conclusions are derived:

1) The technique of strengthening corroded RC columns with combined CFRP sheets and steel jacketing or with steel jacketing alone is quite effective, which significantly increases the strength, ductility and energy absorption and dissipation capacities of the strengthened column, but strengthening a corroded RC column with combined CFRP sheets and steel jacketing is more effective than strengthening only with steel jacketing in improving the strength, ductility and energy absorption and dissipation capacities.

2) The degree of corrosion has a considerable influence on the behavior of the strengthened columns. The strengthening effects of the specimen with a greater degree of corrosion in the ductility is better than those with a lower degree of corrosion.

3) Compared the specimens strengthened with steel jacketing only and those strengthened with combined CFRP and steel jacketing, the CFRP sheet wraps significantly improve the seismic behavior of the strengthened columns.

4) High axial load results in considerable reduction in the ductility of the strengthened columns. The strengthening effect of the columns under low axial load is lower in ductility than that of the columns under high axial load.

5) The yield force, the maximum lateral load and the displacement ductility factor of the strengthened columns can be calculated by the proposed formulae in this paper. A good agreement between calculated values and experimental results is observed.

## References

[1] Shi Qingxuan, Niu Ditao, Yan Guiyun. Experimental research on hysteretic characteristics of corroded RC members with flexural and compressive axial loads under repeated horizontal loading[J]. *Earthquake Engineering and Engineering Vibration*, 2000, **20**(4): 44 − 50. (in Chinese)

[2] Gong Jinxin, Zhong Weiqiu, Zhao Guofan. Experimental study on low-cycle behavior of corroded reinforced concrete member under eccentric compression[J]. *Journal of Building Structures*, 2004, **25**(5): 92 − 104. (in Chinese)

[3] Niu Ditao, Chen Xinxiao, Wang Xuemin. Experimental study on seismic performance of corroded reinforced concrete members with flexure and compression[J]. *Building Structure*, 2004, **34**(10): 36 − 38. (in Chinese)

[4] Belarbi Abdeldjelil, Bae Sang-Wook. An experimental study on the effect of environmental exposures and corrosion on RC columns with FRP composite jackets[J]. *Composites Part B: Engineering*, 2007, **38**(6): 674 − 684.

[5] Maaddawy T. Behavior of corrosion-damaged RC columns wrapped with FRP under combined flexural and axial loading[J]. *Cement and Concrete Composites*, 2008, **30**(6): 524 − 534.

[6] Lu Yiyan, Chen Shaoxiong, Zhao Guofan. An experimental study on the seismic behavior of reinforced concrete column strengthened with bonded steel hoops and carbon fiber reinforced polymer sheet[J]. *China Civil Engineering Journal*, 2005, **38**(8): 10 − 17. (in Chinese)

[7] Sheikh S A, Yau G. Seismic behavior of concrete columns confined with steel and fiber-reinforced polymers[J]. *ACI Structural Journal*, 2002, **99**(1): 72 – 80.
[8] Zhong Weiqiu, Gong Jinxin. Control method for quick electrochemical corrosion experiment of rebars[J]. *Building Technique Development*, 2002, **29**(4): 28 – 29. (in Chinese)
[9] Wang Guangyuan. *Practical methods of optimum seismic design for engineering structures and systems*[M]. Beijing: China Architecture & Building Press, 2000: 66 – 68. (in Chinese)

# 碳纤维布与钢构套复合加固锈蚀钢筋混凝土柱抗震性能

李金波　　贡金鑫

(大连理工大学海岸和近海工程国家重点实验室, 大连 116024)

**摘要:** 为改善锈蚀钢筋混凝土柱的抗震性能, 利用碳纤维布与角钢对锈蚀柱进行复合抗震加固. 试验共对 12 根试件进行了低周反复加载试验, 研究参量包括钢筋锈蚀程度、轴向荷载、碳纤维布层数和角钢用量. 试验结果表明, 利用碳纤维布和角钢复合加固锈蚀柱可以显著改善锈蚀柱的承载能力、延性和耗能能力. 复合加固后, 加固柱的强度和延性与锈蚀柱相比, 可分别提高 0.9 倍和 1 倍以上. 基于试验结果, 提出了计算加固构件屈服荷载、最大荷载和位移延性系数的简化公式, 计算结果与试验结果极为吻合.

**关键词:** 钢筋混凝土柱; 抗震性能; 锈蚀; 加固; 钢构套; 纤维布; 延性
**中图分类号:** TU375.1